Journal of Magnetism and Magnetic Materials 562 (2022) 169794

Contents lists available at ScienceDirect

Journal of Magnetism and Magnetic Materials

journal homepage: www.elsevier.com/locate/jmmm

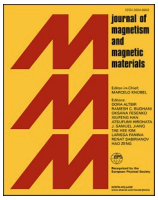

Magnetic properties of α-$KCoPO_4$ compound with a chiral polar crystal structure

J. Kondek, S. Szczupaczyńska-Zalewska, Michal J. Winiarski *

Faculty of Applied Physics and Mathematics and Advanced Materials Center, Gdansk University of Technology, Narutowicza 11/12, 80-233 Gdansk, Poland

A B S T R A C T

We have obtained polycrystalline samples of a metastable α variant of $KCoPO_4$ by low temperature (350–400 °C) solid state metathesis reaction of potassium oxalate and ammonium cobalt orthophosphate. The material crystallizes in a polar chiral structure (sg. $P6_3$, no. 173). Measurements of magnetic properties reveal antiferromagnetic interactions and no ordering observed down to T = 1.9 K, well below the Weiss temperature $|\Theta_{cw}| = 13.9$ K.

1. Introduction

Noncentrosymmetric (NCS) inorganic materials can exhibit various interesting properties. In case of metallic compounds, lack on inversion center can result in exotic triplet superconductivity [1–5]. Noncentrosymmetric insulators can exhibit ferro-, piezo-, and pyroelectric properties, and show nonlinear optical response [6]. In case of magnetic materials, lack of inversion center can result in a complex magnetic structure due to the asymmetric Dzyaloshinskii–Moriya (DM) exchange interaction facilitated by spin-orbit coupling [7–9]. Unusual properties of NCS materials are already employed in electronics as actuators, detectors of movement, pressure and heat in optics, eg. as second harmonic generators. Future applications in magnetic information storage are proposed for NCS magnets hosting the so called skyrmion magnetic texture [10]. However, noncentrosymmetric crystal structures are relatively uncommon among inorganic solids, constituting only about one sixth of all reported structures [11].

The metastable low-temperature chiral polar α-$KCoPO_4$ phase (space group $P6_3$, see Fig. 1(a)) has been reported by Luján, Kubel, and Schmid [12]. It is known to undergo a structural phase transition to the high temperature orthorhombic γ phase (sg. *Pnma*, Fig. 1(b)) around 565 °C [12]. Isotypic α-, and γ-$KZnPO_4$ compounds have also been reported, along with an intermediate temperature polar orthorhombic (sg. $Pna2_1$) β-$KZnPO_4$ variant (the crystal structure of the orthorhombic β variant of $KCoPO_4$ reported by Engel has not been established in detail) [13–17]. A new orthorhombic (s.g $P2_12_12_1$, Fig. 1(c)) variant δ-$KCoPO_4$ was recently synthesized by Yakubovich et al. via a mild hydrothermal method [18]. Relationship between crystal structures of different variants was discussed thoroughly by Yakubovich et al. [18] and by Wallez et al. [16]. $KZnPO_4$ and $KCoPO_4$ belong to a wide family of alkali metal - transition metal phosphates A*TM*PO_4 exhibiting rich structural chemistry and physicochemical properties interesting eg. in terms of energy storage and catalysis [19–21].

To date, magnetic properties were reported only for the δ-$KCoPO_4$ compound, which was found to exhibit antiferromagnetic interactions between the Co^{2+} magnetic moments and a magnetic phase transition around T = 25 K [18]. For the α-$KCoPO_4$, dielectric and magnetoelectric properties were measured down to T = 4.2 K [22], but to the best of our knowledge its magnetic behavior was not described to date.

2. Materials and methods

Polycrystalline α-$KCoPO_4$ (sg. $P6_3$) was prepared by a low-temperature reaction of potassium oxalate monohydrate (Alfa Aesar, ACS grade) and ammonium cobalt phosphate monohydrate (Onyxmet, pure). Reagents were taken in stoichiometric amounts and well ground. The powder was pressed into pellets, put into alumina crucibles, and slowly heated subsequently to 350 °C, 380 °C, and 400 °C with 12 h annealing at each step and an intermediate re-grinding. After heating at 380 °C the sample was found to be phase pure, and further heating only slightly improved its crystallinity (see Fig. S2 of the Supplementary Material for the comparison of powder XRD patterns).

Polycrystalline sample of the isostructural α-$KZnPO_4$ (sg. $P6_3$) was synthesized by precipitation method. The form of the compound that precipitates out of aqueous solution of Zn^{2+} salts and potassium phosphates depends on the solution pH [14,17,23]. The α-$KZnPO_4$ is reported to form at pH between 5 and 7, while above pH = 7 precipitation yields the orthorhombic δ-$KZnPO_4$ [17]. Therefore to prevent the formation of

* Corresponding author.
E-mail address: michal.winiarski@pg.edu.pl (M.J. Winiarski).

https://doi.org/10.1016/j.jmmm.2022.169794
Received 20 May 2022; Received in revised form 4 July 2022; Accepted 4 August 2022
Available online 8 August 2022

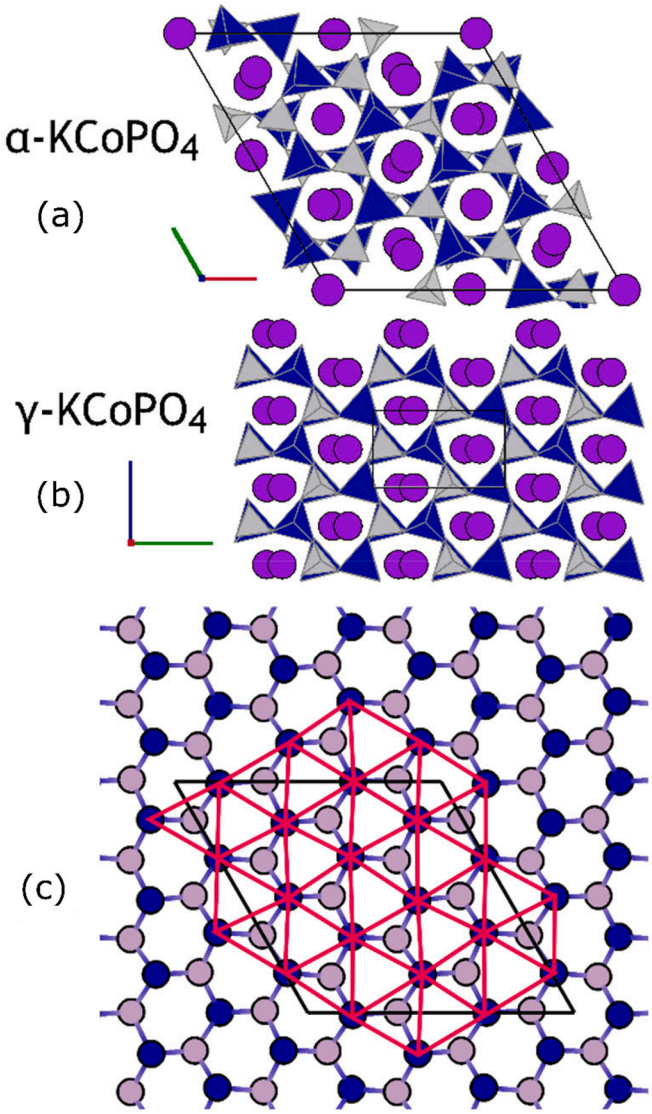

Fig. 1. (a,b) The α and γ structural variants of $KCoPO_4$ differing in stacking of the tetrahedral networks of CoO_4-PO_4. Panel (c) shows the triangular network formed by Co^{2+} cations in the α variant. For the comparison of all reported structural variants of $KCoPO_4$ see the Supplementary Information Fig. S1.

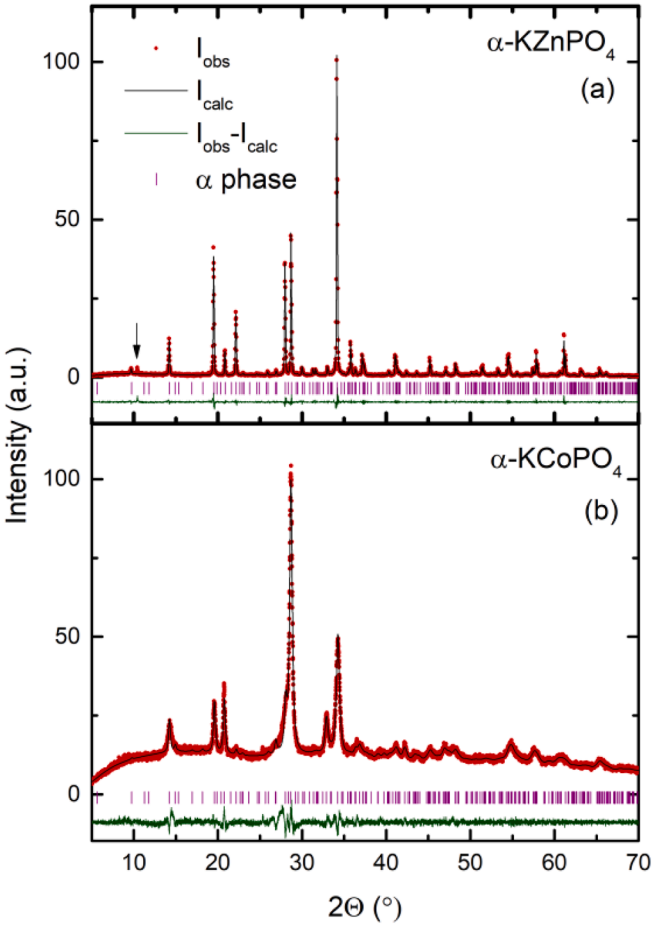

Fig. 2. Powder XRD patterns of (a) α-$KZnPO_4$ obtained after hydrothermal recrystallization, (b) α-$KCoPO_4$ obtained after the last step of solid-state metathesis (heating at 400 °C). LeBail fits using a $P6_3$ cell are shown in black. Expected positions of reflections are shown as purple ticks. Green line is the difference between the observed and calculated intensity. See Fig. S4 of the Supplementary Material for Rietveld fit to the same pXRD data. Black arrow on panel (a) shows the position of an impurity peak, most likely associated with a small amount of $K_2Zn(H_2P_2O_7)_2 \cdot 2\ H_2O$ [25].

the δ variant the reaction was done using a 0.1 M potassium phosphate buffer solution, which was prepared by reacting appropriate amounts of potassium carbonate (Alfa Aesar, 99.9 %) with 1 M phosphoric acid and diluting with deionized (DI) water to the final concentration. The resulting buffer had pH = 6.2. To reduce the amount of dissolved carbon dioxide the buffer solution was degassed by repeated rapid reduction of pressure using a vacuum pump.

A 0.1 M solution of $ZnCl_2$ was prepared by dissolving anhydrous zinc chloride (Alfa Aesar, 98+%) in DI water. The solution was acidified by adding a droplet of concentrated hydrochloric acid to promote solubility by reversing the hydrolysis of $ZnCl_2$ due to a reaction with moisture.

Finally, 25 mL of 0.1 M $ZnCl_2$ solution was added dropwise to 100 mL of the potassium buffer solution. Throughout the reaction the pH was monitored using pH meter and was found to be stable. 10 mL of the resulting white suspension was pipetted to a Teflon-lined autoclave in which it was heated for 1 day at 120 °C. After heating the powder was filtered and dried in air at 120 °C.

Powder X-ray diffraction (XRD) patterns were collected using a Bruker D2 Phaser diffractometer with Cu K_α source and a LynxEye XE-T detector. Rietveld refinement method was used to analyze pXRD data employing the Bruker Topas software.

Measurements of magnetic susceptibility, heat capacity and resistivity were performed using Quantum Design PPMS. Magnetic susceptibility results were obtained with the VSM option. Heat capacity measurements were performed with standard 2τ relaxation method. Heat capacity data for α-$KZnPO_4$ was analyzed using the automated workflow available in the *Materials, Automated* project [24].

3. Results

Analysis of pXRD patterns (Fig. 2 and Fig. S3 of the Supplementary Material) show that as-precipitated α-$KZnPO_4$ is poorly crystallized, but hydrothermal treatment results in a well crystallized polycrystalline powders (Fig. 2(a)). In case of α-$KCoPO_4$ the solid state metathesis reaction yields a phase-pure crystalline product at 380 °C. Rather broad reflections suggests the presence of some atomic disorder due to the low temperature of synthesis. Results of Rietveld refinement show that α-$KCoPO_4$ sample is single phase and free from both observable amounts of other allotropic forms and crystalline impurities, while α-$KZnPO_4$ contains a small amount of an impurity phase, likely $K_2Zn(H_2P_2O_7)_2 \cdot 2\ H_2O$ [25]. Detailed structural parameters resulting from LeBail and Rietveld refinements are given in Tables S1-S2 of the Supplementary Material.

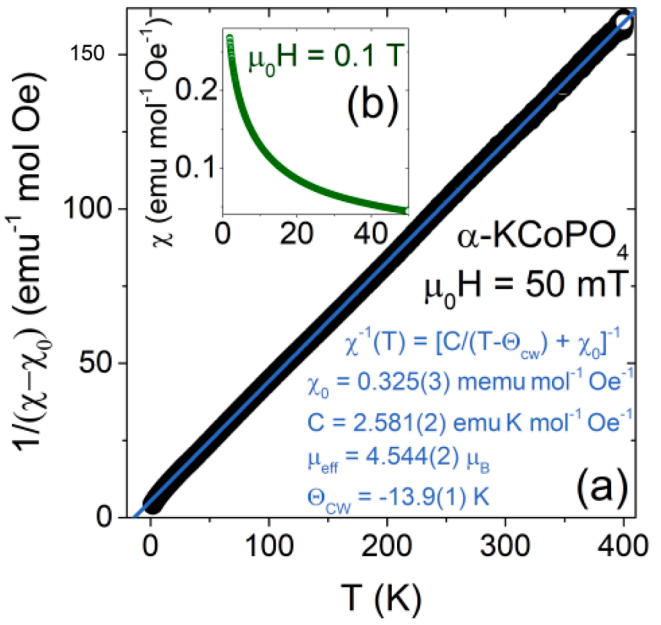

Fig. 3. (a) temperature-dependent inverse susceptibility $\chi^{-1}(T)$ of α-$KCoPO_4$ at $\mu_0H = 50$ mT (black points) along with a fit to the Curie-Weiss law (blue line). Resulting values of temperature-independent susceptibility term, Curie constant, and Weiss temperature are listed in blue. Panel (b) shows low-temperature susceptibility at $\mu_0H = 0.1$ T. No magnetic phase transition is observed down to T = 1.9 K. Numbers in parentheses are statistical uncertainties of the least significant digits.

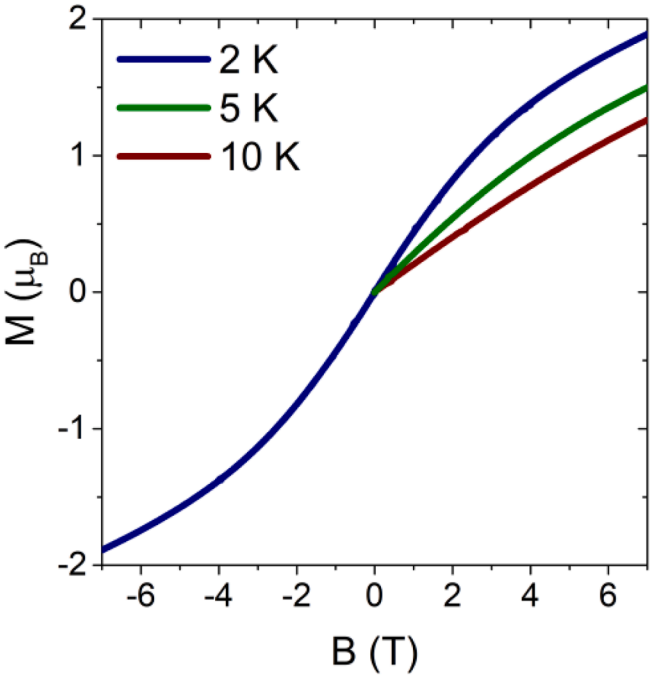

Fig. 4. Field-dependent magnetization of α-$KCoPO_4$ at T = 2.0, 5.0, and 10 K. Magnetization does not saturate at the highest applied field of $\mu_0H = 7$ T.

Magnetization measurements of α-$KCoPO_4$ reveal no sign of long range ordering down to T = 1.9 K (Fig. 3(a,b)). Lujan et al. [22], based on magnetoelectric coupling measurements, reported that at T = 4.4 K the magnetic symmetry must either belong to the antiferromagnetic point group 6′ or the paramagnetic 61′. The lack of magnetic ordering seen in our magnetization and heat capacity data is consistent with the

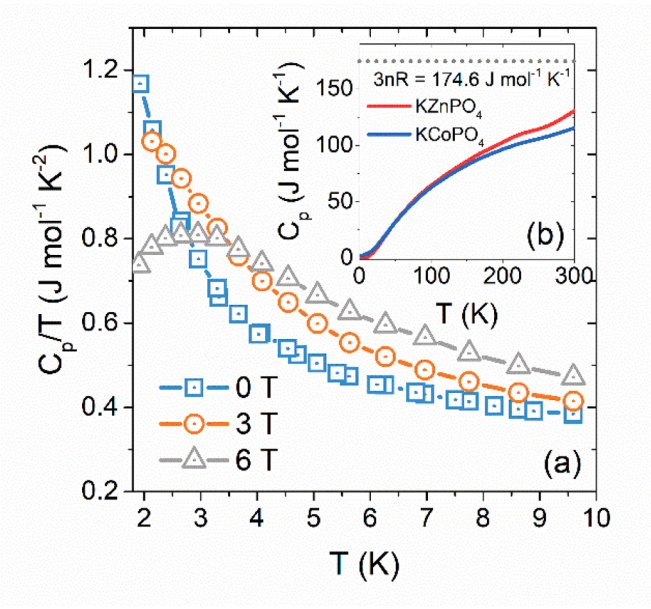

Fig. 5. (a) Low-temperature heat capacity of α-$KCoPO_4$ showing an upturn due to the Schottky anomaly. Panel (b) shows the heat capacity of α-$KCoPO_4$ and α-$KZnPO_4$ in the full measured temperature range 1.9 K < T < 300 K. The Dulong-Petit limit is shown with dashed gray line. Fig. S5 of the Supplementary Information shows low-temperature heat capacity α-$KCoPO_4$ in $\mu_0H = 0$, 2, 4, 6, 8 T.

latter.

Magnetic susceptibility in a wide temperature range follows the Curie-Weiss law:

$$\chi(T) = \frac{C}{T - \Theta_{CW}} + \chi_0$$

A fit of the inverse susceptibility at an applied field $\mu_0H = 7$ T (Fig. 3 (a)) yields $\chi_0 = 0.325(3)$ memu mol^{-1} Oe^{-1}. The Weiss temperature $\Theta_{CW} = -13.9(1)$ K, suggests the presence of antiferromagnetic interactions between Co^{2+} moments, and the Curie constant C = 2.684(1) emu K / mol Oe, equivalent to an average effective moment of $\mu_{eff} = 4.544(2)\ \mu_B$ per cobalt ion. The effective moment is significantly higher than a spin only value of $\mu_{eff} = \sqrt{4S(S+1)} = 3.873\mu_B$, indicating a significant orbital contribution, typical for tetrahedral Co^{2+} systems [26,27].

Since no magnetic ordering was observed down to T = 1.9 K, it is only possible to estimate the lower limit of the frustration index *f*:

$$f = \frac{|\Theta_{CW}|}{T_t}$$

Where in our case the transition temperature T_t is replaced with the lowest temperature reached in the susceptibility measurement $T_{low} = 1.9$ K. This yields $f \geq 7.3$, indicative of magnetic frustration [28]. This is in contrast to the behavior of the δ-$KCoPO_4$ variant which exhibits magnetic transition at T = 25 K, close to the value of its Weiss temperature $|\Theta_{CW}| = 26$ K [18].

The field-dependent magnetization M(H) data shows a nonlinear behavior (Fig. 4), consistent with a paramagnetic state at low temperatures and high fields. At T = 2.0 K and in an applied field $\mu_0H = 7.0$ T does not reach saturation (expected at 3 μ_B for a spin-only case).

Heat capacity of α-$KCoPO_4$ (Fig. 5(a)) shows a sharp upturn at the low-temperature limit. The anomaly is shifted to higher temperatures by the application of magnetic field. Such behavior (Schottky anomaly) is expected for a paramagnetic system at low temperatures [29]. At T = 300 K both the Co- and Zn- bearing compound do not reach the Dulong-Petit limit, in consistency with the presence of high frequency phonon

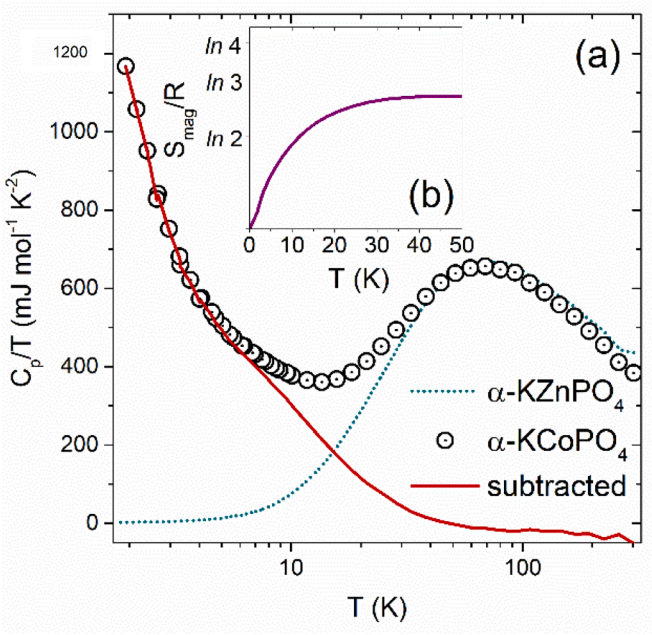

Fig. 6. (a) Heat capacity of α-$KCoPO_4$ (points) and α-$KZnPO_4$ (blue dotted line). Magnetic heat capacity of the former (red line) is estimated by subtracting heat capacity of the non-magnetic isostructural α-$KZnPO_4$. Inset (b) shows the magnetic entropy S_{mag} of α-$KCoPO_4$ calculated by integrating the magnetic heat capacity C_{mag}.

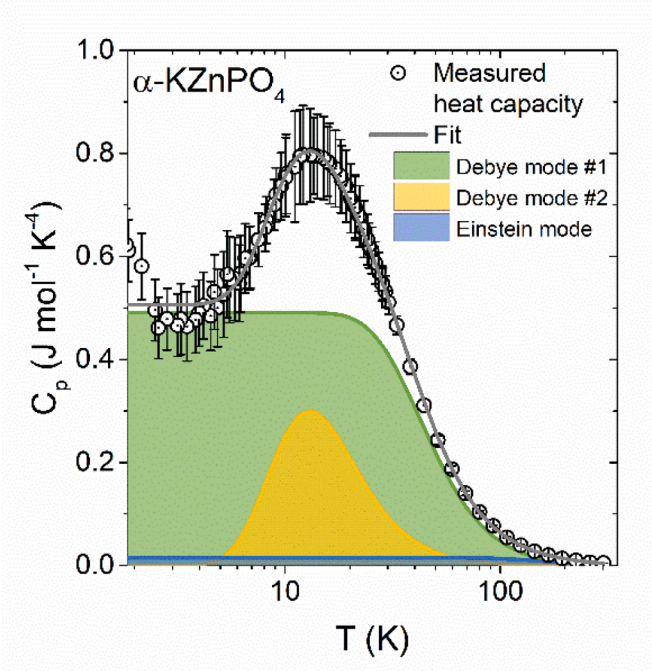

Fig. 7. Fit to the heat capacity of α-$KZnPO_4$ using a model with two Debye and one Einstein oscillators with refined characteristic temperatures and degeneracies.

modes. A slightly higher value of room temperature heat capacity of α-$KZnPO_4$ compared to α-$KCoPO_4$ might be caused by a lower average phonon frequency due to the difference in mass between Zn and Co. The difference can also be partially caused by the small amount of an impurity phase seen in the XRD pattern (see Fig. 2).

For the nonmagnetic compound α-$KZnPO_4$ the heat capacity (C_p) shows no anomaly down to T = 1.9 K (Fig. 6(a)). The magnetic contribution to the heat capacity of α-$KCoPO_4$ (C_{mag}) was estimated by subtracting the measured C_p of α-$KZnPO_4$. Integration of C_{mag}/T vs T yields magnetic entropy S_{mag} (Fig. 6(b)), which saturates at T = 50 K to the value slightly less than R ln 3. This is significantly lower than expected for a S = 3/2 system (R ln 4), most likely due to the insufficient range of low-temperature measurements.

Heat capacity of α-$KZnPO_4$ (Fig. 7) was fitted with a model consisting of two Debye and one Einstein oscillators (both mode temperatures and degeneracies were allowed to vary). This yields Debye temperatures Θ_{D1} = 209(1) K and Θ_{D2} = 770(10) K and Einstein temperature Θ_E = 64.0(5) K with mode degeneracy of 2.31(3), 3.50(5), and 0.148(4), respectively. The total number of oscillators is thus roughly equal to 5 while the formula unit contains 7 atoms. This discrepancy likely stems from the presence of high frequency optical modes (with characteristic temperatures well above Θ = 300 K). This is consistent with the heat capacity at T = 300 K being significantly lower than the Dulong-Petit limit (see Fig. 5(b)).

4. Conclusions

We described the synthesis and magnetic characterization of the chiral magnet α-$KCoPO_4$. The compound was found to show frustrated antiferromagnetic interactions (Weiss temperature Θ_{CW} = −13.9(1) K) but no magnetic transition was observed down to T = 1.9 K. This is in contrast with the behavior of the recently reported orthorhombic δ variant, which shows no appreciable magnetic frustration.

The investigated compound α-$KCoPO_4$ is a member of a compositionally and structurally rich A*TM*PO_4 family (*A* – alkali cation or ammonium, *TM* – transition metal), in which various magnetic ground states can arise due to interplay of crystal structure and *d* orbital filling [30–38]. Polymorphism found in many of the A*TM*PO_4 compounds makes them an interesting object of studying the structure-properties relationship.

CRediT authorship contribution statement

J. Kondek: Investigation, Formal analysis, Visualization, Writing – original draft. **S. Szczupaczyńska-Zalewska:** Investigation, Formal analysis, Visualization, Writing – original draft. **M.J. Winiarski:** Conceptualization, Funding acquisition, Resources, Supervision, Visualization, Writing – original draft, Writing – review & editing.

Declaration of Competing Interest

The authors declare that they have no known competing financial interests or personal relationships that could have appeared to influence the work reported in this paper.

Data availability

Data will be made available on request.

Acknowledgements

The research was supported by the National Science Centre (Poland) under SONATA-15 grant (UMO- 2019/35/D/ST5/03769).

Appendix A. Supplementary material

Supplementary data to this article can be found online at https://doi.org/10.1016/j.jmmm.2022.169794.

References

[1] L.P. Gor'kov, E.I. Rashba, Superconducting 2D System with Lifted Spin Degeneracy: Mixed Singlet-Triplet State, Phys. Rev. Lett. 87 (3) (2001), 037004, https://doi.org/10.1103/PhysRevLett.87.037004.

[2] S. Yip, Noncentrosymmetric Superconductors, Annu. Rev. Condens. Matter Phys. 5 (2014) 15–33, https://doi.org/10.1146/annurev-conmatphys-031113-133912.

[3] E. Bauer, M. Sigrist, Non-Centrosymmetric Superconductors: Introduction and Overview, Springer Science & Business Media, 2012.

[4] E.M. Carnicom, W. Xie, T. Klimczuk, J. Lin, K. Górnicka, Z. Sobczak, N.P. Ong, R. J. Cava, TaRh 2 B 2 and NbRh2B2: Superconductors with a chiral noncentrosymmetric crystal structure, Sci. Adv. 4 (2018) eaar7969, https://doi.org/10.1126/sciadv.aar7969.

[5] K. Górnicka, X. Gui, B. Wiendlocha, L.T. Nguyen, W. Xie, R.J. Cava, T. Klimczuk, NbIr2B2 and TaIr2B2 – New Low Symmetry Noncentrosymmetric Superconductors with Strong Spin-Orbit Coupling, Adv. Funct. Mater. 31 (2021) 2007960, https://doi.org/10.1002/adfm.202007960.

[6] P.S. Halasyamani, K.R. Poeppelmeier, Noncentrosymmetric Oxides, Chem. Mater. 10 (1998) 2753–2769, https://doi.org/10.1021/cm980140w.

[7] I. Kézsmárki, S. Bordács, P. Milde, E. Neuber, L.M. Eng, J.S. White, H.M. Rønnow, C.D. Dewhurst, M. Mochizuki, K. Yanai, H. Nakamura, D. Ehlers, V. Tsurkan, A. Loidl, Néel-type skyrmion lattice with confined orientation in the polar magnetic semiconductor GaV4S8, Nat. Mater. 14 (2015) 1116–1122, https://doi.org/10.1038/nmat4402.

[8] S. Seki, M. Garst, J. Waizner, R. Takagi, N.D. Khanh, Y. Okamura, K. Kondou, F. Kagawa, Y. Otani, Y. Tokura, Propagation dynamics of spin excitations along skyrmion strings, Nat. Commun. 11 (2020) 256, https://doi.org/10.1038/s41467-019-14095-0.

[9] E.E. Oyeka, M.J. Winiarski, A. Błachowski, K.M. Taddei, A. Scheie, T.T. Tran, Potential Skyrmion Host Fe(IO3)3: Connecting Stereoactive Lone-Pair Electron Effects to the Dzyaloshinskii-Moriya Interaction, Chem. Mater. 33 (2021) 4661–4671, https://doi.org/10.1021/acs.chemmater.1c01163.

[10] A. Fert, N. Reyren, V. Cros, Magnetic skyrmions: advances in physics and potential applications, Nat. Rev. Mater. 2 (2017) 1–15, https://doi.org/10.1038/natrevmats.2017.31.

[11] D.V. West, I.D. Posen, Q. Huang, H.W. Zandbergen, T.M. McQueen, R.J. Cava, PbMn(SO4)2: A new chiral antiferromagnet, J. Solid State Chem. 182 (2009) 2461–2467, https://doi.org/10.1016/j.jssc.2009.06.021.

[12] M.L. Lujan Perez, F. Kubel, H. Schmid, Crystal growth and x-ray structure of metastable a-$KCoPO_4$, Zeitschrift Für Naturforschung. B. 49 (1994) 1256.

[13] G. Engel, Untersuchungen zur kristallchemie verschiedener phosphate namiipo4 und verwandter verbindungen, Neues Jahrbuch Fuer Mineralogie, Abhandlungen. 127 (1976) 197–211.

[14] Thierry Barbou des Courières, Marie-Hélène Simonot-Grange, KZn2H(PO4)2 2.5H2O II. Instability. Characterization of new, mixed zinc and potassium phosphates, Mater. Res. Bull. 14 (11) (1979) 1419–1424.

[15] M. Andratschke, K.-J. Range, H. Haase, U. Klement, Die Kristallstruktur von α-KZnPO4 / The Crystal Structure of α-KZnPO4, Zeitschrift Für Naturforschung B. 47 (1992) 1249–1254, https://doi.org/10.1515/znb-1992-0906.

[16] G. Wallez, F. Lucas, J.-P. Souron, M. Quarton, Potassium-zinc monophosphate: an original polymorphic tridymite derivate, Mater. Res. Bull. 34 (1999) 1251–1261, https://doi.org/10.1016/S0025-5408(99)00124-5.

[17] Peter G. Self, Mark D. Raven, Characterization of δ-KZnPO4 by X-ray powder diffraction, Powder Diffr. 36 (4) (2021) 257–261.

[18] O.V. Yakubovich, L.V. Shvanskaya, N.B. Bolotina, A.G. Ivanova, G.V. Kiriukhina, I. N. Dovgaliuk, A.S. Volkov, O.V. Dimitrova, A.N. Vasiliev, An Orthorhombic Modification of KCoPO4 Stabilized under Hydrothermal Conditions: Crystal Chemistry and Magnetic Behavior, Inorg. Chem. 60 (2021) 9461–9470, https://doi.org/10.1021/acs.inorgchem.1c00580.

[19] A.K. Padhi, K.S. Nanjundaswamy, J.B. Goodenough, Phospho-olivines as Positive-Electrode Materials for Rechargeable Lithium Batteries, J. Electrochem. Soc. 144 (4) (1997) 1188–1194.

[20] H. Zhao, Z.-Y. Yuan, Insights into Transition Metal Phosphate Materials for Efficient Electrocatalysis, ChemCatChem 12 (2020) 3797–3810, https://doi.org/10.1002/cctc.202000360.

[21] P.F. Henry, M.T. Weller, R.W. Hughes, Nickel Phosphate Based Zeotype, RbNiPO4, Inorg. Chem. 39 (2000) 5420–5421, https://doi.org/10.1021/ic000712q.

[22] M. Luján, J.-P. Rivera, H. Schmid, Synthesis and magnetoelectric properties of single crystals of metastable KCoPO4, Ferroelectrics 162 (1994) 69–80, https://doi.org/10.1080/00150199408245092.

[23] A.W. Frazier, J.P. Smith, J.R. Lehr, Precipitated Impurities of Fertilizers Prepared from Wet-Process Phosphoric Acid, J. Agric. Food Chem. 14 (1966) 522–529, https://doi.org/10.1021/jf60147a026.

[24] Materials, Automated. https://materialsautomated.github.io/ (accessed November 29, 2021).

[25] R. Essehli, B. El Bali, A. Alaoui Tahiri, M. Lachkar, B. Manoun, M. Dušek, K. Fejfarova, K2M(H2P2O7)2·2H2O (M = Ni, Cu, Zn): orthorhombic forms and Raman spectra, Acta Cryst C. 61 (2005) i120–i124, https://doi.org/10.1107/S0108270105036656.

[26] F.A. Cotton, D.M.L. Goodgame, M. Goodgame, The Electronic Structures of Tetrahedral Cobalt(II) Complexes, J. Am. Chem. Soc. 83 (1961) 4690–4699, https://doi.org/10.1021/ja01484a002.

[27] C. Decaroli, A.M. Arevalo-Lopez, C.H. Woodall, E.E. Rodriguez, J.P. Attfield, S. F. Parker, C. Stock, (C4H12N2)[CoCl4]: tetrahedrally coordinated Co2+ without the orbital degeneracy, Acta Cryst B. 71 (2015) 20–24, https://doi.org/10.1107/S2052520614024809.

[28] A.P. Ramirez, Strongly Geometrically Frustrated Magnets, Annu. Rev. Mater. Sci. 24 (1994) 453–480, https://doi.org/10.1146/annurev.ms.24.080194.002321.

[29] R.L. Carlin, Thermodynamics, in: R.L. Carlin (Ed.), Magnetochemistry, Springer, Berlin, Heidelberg, 1986, pp. 36–51. https://doi.org/10.1007/978-3-642-70733-9_3.

[30] P. Fischer, M. Luján, F. Kubel, H. Schmid, Crystal structure and magnetic ordering in magnetoelectric KNiPO4 investigated by means of X-ray and neutron diffraction, Ferroelectrics 162 (1994) 37–44, https://doi.org/10.1080/00150199408245088.

[31] P. Feng, X. Bu, S.H. Tolbert, G.D. Stucky, Syntheses and Characterizations of Chiral Tetrahedral Cobalt Phosphates with Zeolite ABW and Related Frameworks, J. Am. Chem. Soc. 119 (1997) 2497–2504, https://doi.org/10.1021/ja9634841.

[32] P. Feng, X. Bu, G.D. Stucky, Synthesis and Characterizations of a Polymorphic Sodium Cobalt Phosphate with Edge-Sharing Co2+ Octahedral Chains, J. Solid State Chem. 131 (1997) 160–166, https://doi.org/10.1006/jssc.1997.7390.

[33] M.T. Weller, Where zeolites and oxides merge: semi-condensed tetrahedral frameworks, J. Chem. Soc., Dalton Trans. (2000) 4227–4240, https://doi.org/10.1039/B003800H.

[34] M. Ulutagay-Kartin, K.M.S.G. Etheredge, G.L. Schimek, S.-J. Hwu, Synthesis, structure, and magnetic properties of two quasi-low-dimensional antiferromagnets, NaMnAsO4 and β-NaCuPO4, J. Alloy. Compd. 338 (2002) 80–86, https://doi.org/10.1016/S0925-8388(02)00242-6.

[35] Gwilherm Nénert, Jerry Bettis, Reinhard Kremer, Hamdi Ben Yahia, Clemens Ritter, Etienne Gaudin, Olivier Isnard, Myung-Hwan Whangbo, Magnetic Properties of the RbMnPO4 Zeolite-ABW-Type Material: A Frustrated Zigzag Spin Chain, Inorg. Chem. 52 (16) (2013) 9627–9635.

[36] M. Avdeev, Z. Mohamed, C.D. Ling, J. Lu, M. Tamaru, A. Yamada, P. Barpanda, Magnetic Structures of NaFePO4 Maricite and Triphylite Polymorphs for Sodium-Ion Batteries, Inorg. Chem. 52 (2013) 8685–8693, https://doi.org/10.1021/ic400870x.

[37] I.V. Korchemkin, V.I. Pet'kov, A.V. Markin, N.N. Smirnova, A.M. Kovalsky, N. N. Efimov, V.M. Novotortsev, Thermodynamic properties of caesium–manganese phosphate CsMnPO4, J. Chem. Thermodyn. 78 (2014) 114–119.

[38] S. Jana, G. Lingannan, M. Ishtiyak, G. Panigrahi, A. Sonachalam, J. Prakash, Syntheses, crystal structures, optical, Raman spectroscopy, and magnetic properties of two polymorphs of NaMnPO4, Mater. Res. Bull. 126 (2020), 110835, https://doi.org/10.1016/j.materresbull.2020.110835.